J Mater Sci (2008) 43:4450–4454
DOI 10.1007/s10853-008-2656-4

Effect of the addition of t-ZrO_2 on the material properties of β-TCP/PCL composites

Ho-Yeon Song · Do Van Quang · Young-Ki Min · Byong-Taek Lee

Received: 16 January 2008 / Accepted: 14 April 2008 / Published online: 29 April 2008

Abstract Using poly-methyl methacrylate as a pore-forming agent, porous β-tricalcium phosphate (β-TCP)/t-ZrO_2 composites were fabricated depending on the volume percentages (vol.%) of t-ZrO_2 powder. In the porous sintered bodies, hybrid pores, about 20 and 200 μm in diameter, were homogenously dispersed in the β-TCP/t-ZrO_2 matrix and showed good interconnection. On the other hand, β-TCP-(t-ZrO_2)/polycaprolactone (PCL) composites were fabricated by the melt infiltration process using porous β-TCP/t-ZrO_2 bodies. The relative density of the β-TCP-(t-ZrO_2)/PCL composites increased as the vol.% of t-ZrO_2 increased and its maximum value was about 98.6%. However, the hardness, bending strength and elastic modulus of β-TCP-(t-ZrO_2)/PCL composites decreased due to the low densification of porous β-TCP/t-ZrO_2 bodies as the volume percentages of t-ZrO_2 content increased. The values (using 20 vol.% of t-ZrO_2) were 11.4 Hv, 25.5 MPa and 17.2 GPa, respectively.

Introduction

β-Tricalcium phosphates (β-$Ca_3(PO_4)_2$, β-TCP) have been widely used as biomaterials for bone substitutes [1–3] because their chemical composition is similar to that of human bone and teeth. Moreover, β-TCP has some unique properties such as excellent biocompatibility and osteo-integration [4]. Its high potential for resorption in the human biological environment allows a significant recovery of the operational site by advancing bone growth during the progressive degradation of this material [5]. However, β-TCP has poor mechanical properties, such as low fracture strength and low fracture toughness compared to human bone. On the other hand, polycaprolactone (PCL) has been used for bone substitutes and as a drug carrier because of its typical biodegradable property with excellent biocompatibility [6, 7].

In previous work, BCP/PCL composites were successfully fabricated by infiltration of molten PCL into porous BCP bodies, using 70 vol.% of poly-methyl methacrylate (PMMA) powder as a pore-forming agent (about 200 μm in diameter). However, when the percentage of PMMA powder was increased to 80 vol.%, the porous bodies were quite weak and broke easily during the infiltration process of molten PCL. Therefore, to make sound β-TCP-(t-ZrO_2)/PCL composites, porous β-TCP bodies using 80 vol.% of PMMA powder should be reinforced to keep their original shape during the infiltration process. Recently, yttria (3 mol%) stabilized zirconia (t-ZrO_2) has received a lot of attention for artificial implants due to its biocompatibility and corrosion resistance, high fracture toughness, excellent chemical stability and outstanding mechanical properties [8–10]. Hence, t-ZrO_2 is considered to be one of the most suitable reinforcements for porous β-TCP bodies.

In this work, to make porous β-TCP/t-ZrO_2 bodies, hybrid PMMA powders (20 and 200 μm in diameter) were used as a pore-forming agent. Then, using the melt infiltration process, the molten PCL was infiltrated into the porous β-TCP/t-ZrO_2 bodies to obtain the β-TCP-(t-ZrO_2)/PCL composites.

Experimental procedure

As starting materials, biphasic calcium phosphate (BCP) powders (about 80 nm) were synthesized by a microwave-

H.-Y. Song · D. Van Quang · Y.-K. Min · B.-T. Lee (✉)
Department of Biomedical Engineering and Materials, School of Medicine, Soonchunhyang University, 366-1, Ssangyoung-dong, Cheonan, Chungnam 330-090, South Korea
e-mail: lbt@sch.ac.kr

assisted process [11]. Spherical t-ZrO_2 powder (about 70 nm, Tosoh, Japan) and PMMA powders (about 20 and 200 μm in diameter, LG chemical company, Korea) as a pore-forming agent were used. First, BCP and different volume percentages (20, 30, 40, 50 vol.%) of t-ZrO_2 powders were mixed for 24 h by wet-ball milling using Al_2O_3 balls. Then, the mixture powders were dried on a hot plate while stirring. The BCP/t-ZrO_2 powders and 80 vol.% of PMMA powders (20 and 200 μm in diameter) were mixed for 15 h by dry-ball milling also using Al_2O_3 balls. The mixture powders after dry-ball milling were compacted into pellets by a uni-axial press and were burned out in an air atmosphere at 700 °C. Finally, the burn-out samples were sintered at 1,400 °C in an air atmosphere.

On the other hand, PCL (Aldrich, USA) was melted at 120 °C, and then poured into a mold containing porous β-TCP/t-ZrO_2 bodies. They were kept at the same melt temperature of the PCL for about 5–10 min before natural cooling. After complete solidification of the melted PCL, the PCL on the outside of the samples was removed to take β-TCP-(t-ZrO_2)/PCL composites.

The relative density of β-TCP-(t-ZrO_2)/PCL composites was measured by the Archimedes method. The pore size and microstructure of the porous β-TCP/t-ZrO_2 bodies and β-TCP-(t-ZrO_2)/PCL composites were investigated by scanning electron microscopy (SEM, JSM-635F, Jeol). To identify the crystal structure and phases, an X-ray diffractometer (XRD, D/MAX-250, Rigaku, Japan) were used. The hardness was measured using a Vickers hardness tester (Hv-112, Akashi, Japan) by indentation with a load of 0.3 kg (10 points/sample). For bending strength and elastic modulus measurements, the samples were bar-shaped ($4 \times 4 \times 35$ mm^3). The bending strength measurement was carried out using a four-point bending method with a span of 10 mm and a crosshead speed of 0.1 mm/min, using a universal testing machine (Unitech^{TM}, R&B, Korea). The elastic modulus was calculated using the following equation, which was developed by Grindosonic (J. W. Lemmens, MKS) [12].

$$E_R = 0.9465 * \frac{M * f^2}{w} * \frac{L_T^3}{t^3} * \left[1 + 6.59 * \left(\frac{t^2}{L_T^2}\right)\right]$$

where E_R is the elastic modulus, M is the weight, f is the frequency, w is the width, L_T is the length and t is the thickness of the specimen. When the elastic modulus was calculated, average values (15 times) were used.

Results and discussion

Figure 1 shows a SEM micrograph of (a) raw BCP, a TEM micrograph of (b) raw t-ZrO_2 powders, and SEM micrographs of two types of (c) and (d) raw PMMA powders. The particle size of the raw BCP powder was in the range of 70–90 nm in diameter and the particle size of the spherical t-ZrO_2 powder was about 70 nm in diameter. Two types of PMMA powders, which were used together as a pore-forming agent, were spherical-shaped and about 20 and 200 μm in diameter. However, a few small particles of less than 10 μm in diameter were also observed.

Figure 2 shows SEM micrographs of porous β-TCP/t-ZrO_2 bodies depending on the t-ZrO_2 content. In Fig. 2a, containing 50 vol.% t-ZrO_2 powder, large amounts of special homogeneous pores about 200 μm in diameter were observed. From the enlarged image seen in Fig. 2b, it is confirmed that hybrid-type pores were formed in the porous β-TCP/t-ZrO_2 body due to the burn-out of the large (200 μm) and small (20 μm) PMMA powders located at the pore frame. On the surface of the large sized pores and their pore frames, many fine, interconnected pores were observed, which will have beneficial effects on the infiltration of the PCL. On the other hand, Fig. 2c and d show enlarged images of pore frame of porous β-TCP/t-ZrO_2 bodies using 20 and 50 vol.% of t-ZrO_2 powders, respectively. The t-ZrO_2 grains were less than 0.7 μm in diameter and were homogenously dispersed in the β-TCP matrix. However, an important observation was that in the sample containing 20 vol.% t-ZrO_2 powder, a dense microstructure was found, whereas in the sample containing 50 vol.% t-ZrO_2 powder, some fine pores were observed as indicated with arrowheads. This means that the sinterability of porous β-TCP/t-ZrO_2 bodies decreased as the t-ZrO_2 content increased.

Figure 3 shows XRD profiles of (a) burn-out at 700 °C, sintered at 1,400 °C of β-TCP/t-ZrO_2 bodies containing (b) 20 vol.% of t-ZrO_2 and (c) 50 vol.% of t-ZrO_2 powders. In the burned-out sample, BCP containing hydroxyapatite (HAp) and β-TCP phases were detected as well as a t-ZrO_2 phase. However, in the sintered samples, neither HAp nor new reaction phases were found after the sintering process. The intensity of the t-ZrO_2 phase also slightly increased while the β-TCP phase slightly decreased as the t-ZrO_2 content increased.

Figure 4 shows the relative density, hardness, bending strength and elastic modulus of the β-TCP-(t-ZrO_2)/PCL composites depending on the t-ZrO_2 content. The relative density increased as the t-ZrO_2 content increased, and its maximum value was about 98.6%. However, the hardness, bending strength and elastic modulus of the β-TCP-(t-ZrO_2)/PCL composites slightly decreased as the t-ZrO_2 content increased. Using 20 vol.% of t-ZrO_2 content, the values were about 11.4 Hv, 25.5 MPa and 17.2 GPa, respectively. The value of the elastic modulus was controlled in the range of that of cortical bone [13]. As mentioned in Fig. 2d, some fine pores were observed when the t-ZrO_2 content increased. Therefore, after the infiltration process, the fine pores were also infiltrated by PCL,

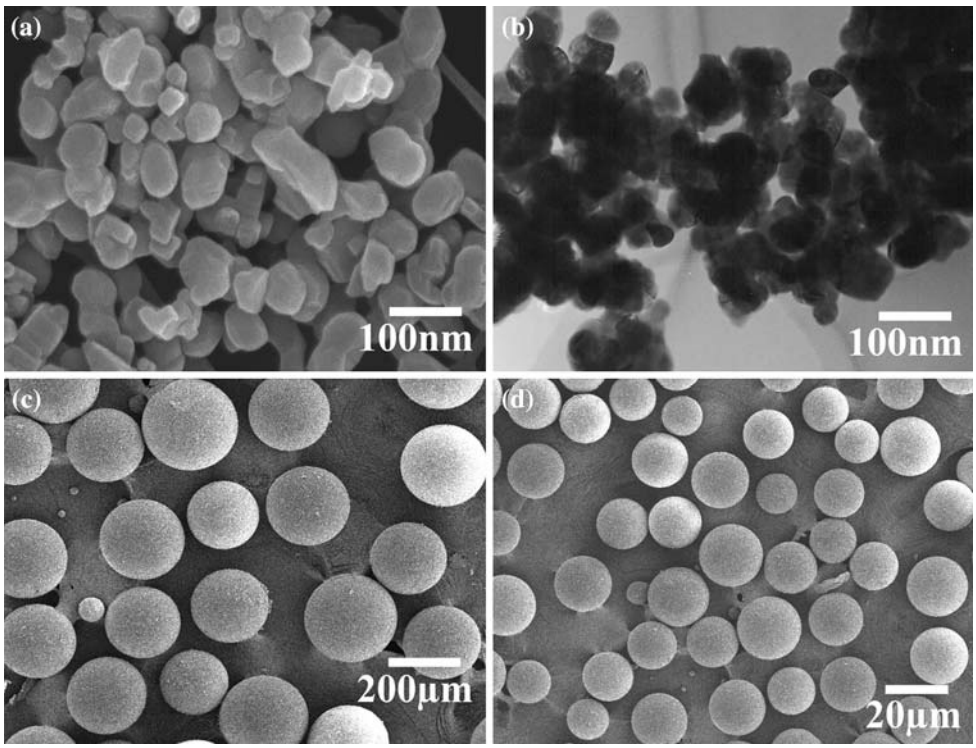

Fig. 1 SEM and TEM micrographs of raw (**a**) BCP, (**b**) t-ZrO_2, (**c**) PMMA (200 μm) and (**d**) PMMA (20 μm) powders

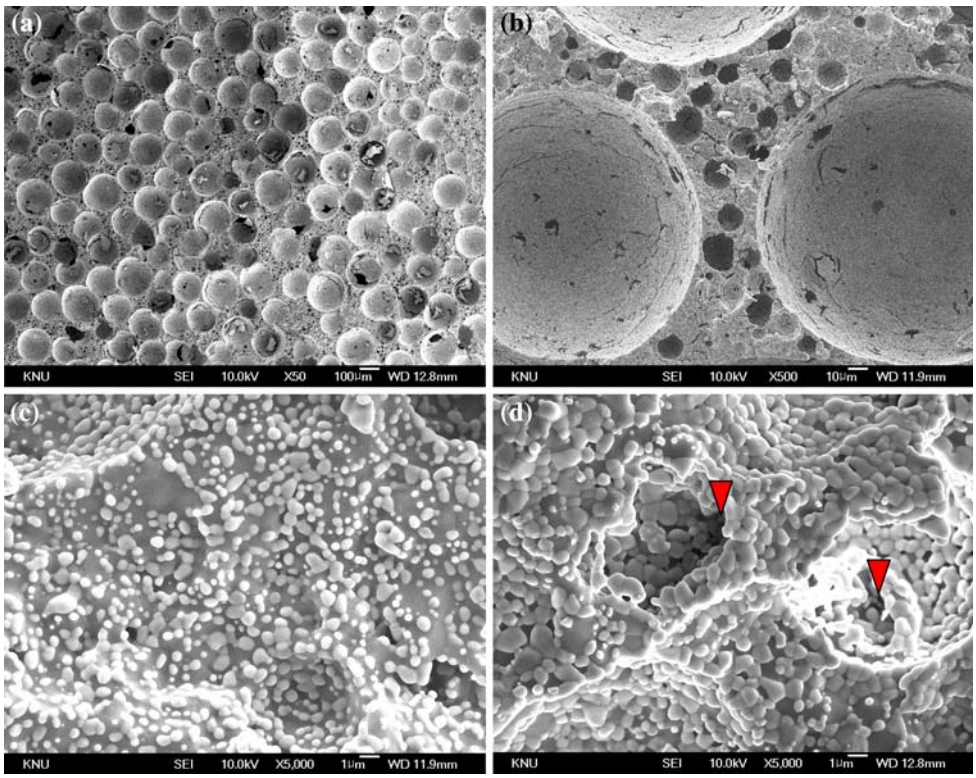

Fig. 2 SEM micrographs of porous β-TCP-(t-ZrO_2) bodies using 50 vol.% of t-ZrO_2 (**a**) low magnification, (**b**) enlarged pore frame, high magnification of pore frame of porous β-TCP-(t-ZrO_2) bodies using (**c**) 20 vol.% of t-ZrO_2 and (**d**) 50 vol.% of t-ZrO_2

which explained why the value of the relative density of the composites increased while the values of hardness, bending strength and elastic modulus of the composites slightly decreased as the vol.% of t-ZrO_2 increased.

Figure 5a and b show SEM micrographs and SEM fracture surfaces of β-TCP-(t-ZrO_2)/PCL composites containing 20 vol.% t-ZrO_2, whereas Fig. 5c–e contain 50 vol.% t-ZrO_2 powders. In Fig. 5a, the dark contrast regions appear

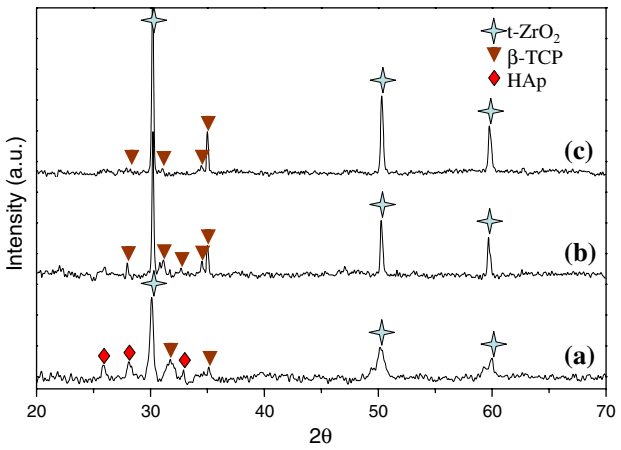

Fig. 3 XRD profiles of (**a**) burn-out at 700 °C, sintering at 1,400 °C of β-TCP-(t-ZrO_2) bodies containing (**b**) 20 vol.% of t-ZrO_2 and (**c**) 50 vol.% of t-ZrO_2

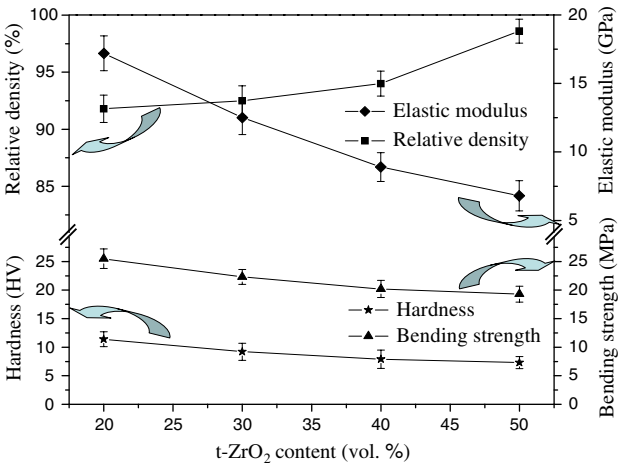

Fig. 4 Relative density, elastic modulus, hardness and bending strength of β-TCP-(t-ZrO_2)/PCL composites depending on the t-ZrO_2 content

with a special shape, which corresponds to the infiltrated PCL phase while the bright regions are β-TCP-(t-ZrO_2) phases. Due to full infiltration of the PCL, the residual pores were hardly observed on the polished sample. In Fig. 5b, the fracture surface was flat and the pulled-out spherical PCL was hardly observed. This observation reveals that the interfaces between β-TCP-(t-ZrO_2)/PCL show comparatively strong bonding. In Fig. 5c, many pulled-out PCL spheres and their traces were observed on the fracture surface of the β-TCP-(t-ZrO_2)/PCL composites although some of the PCL spheres were torn during the fracture. This observation means that the interfacial strength between the β-TCP/t-ZrO_2 frame and PCL spheres was low compared with that of the PCL. In Fig. 5d, which is an enlarged image of Fig. 5c, the gap between the PCL and pore frame was clearly observed, as indicated with an arrow. Figure 5e shows high magnification of the pore frame of Fig. 5c, which is a typical mixed fracture mode, with trans-granular and inter-granular types that frequently appear in brittle ceramics.

Conclusion

Porous β-TCP/t-ZrO_2 bodies were fabricated depending on the vol.% of t-ZrO_2 (20, 30, 40, 50) using 80 vol. % of PMMA as a pore-forming agent. Due to the burn-out and sintering processes, the PMMA was completely removed. In the porous sintered bodies, the pores, about 20 and 200 μm in diameter, were homogenously dispersed in the β-TCP/t-ZrO_2 matrix and showed good interconnection between them. β-TCP-(t-ZrO_2)/PCL composites were fabricated by the melt infiltration process using porous β-TCP/t-ZrO_2 bodies and molten PCL. Most of the β-TCP/t-ZrO_2 pores were fully infiltrated by the molten PCL. As the volume percentage of t-ZrO_2 increased, many pulled-out PCL spheres and their traces were observed on the fracture

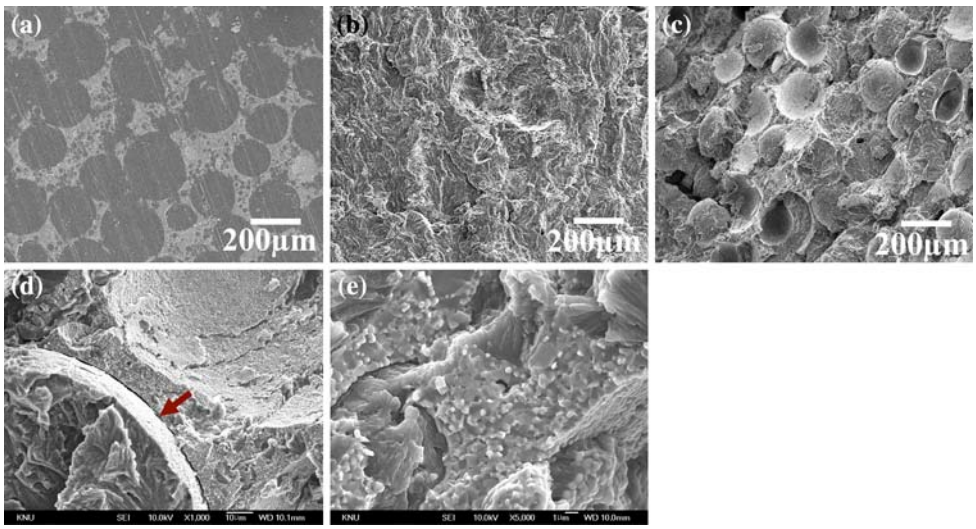

Fig. 5 SEM micrographs of β-TCP-(t-ZrO_2)/PCL composites using 20 vol.% of t-ZrO_2 (**a**) polished surface, (**b**) fracture surface, (**c**) fracture surface of β-TCP-(t-ZrO_2)/PCL composites using 50 vol.% of t-ZrO_2, (**d**) enlarged image of (**c**) and (**e**) high magnification of pore frame of (**c**)

surface. The value of relative density of β-TCP-(t-ZrO_2)/PCL composites increased as the vol.% of t-ZrO_2 increased. However, the values of hardness, bending strength and elastic modulus of β-TCP-(t-ZrO_2)/PCL composites decreased as the vol.% of t-ZrO_2 content increased.

Acknowledgements This research was supported by a grant from the Center for Advanced Materials Processing (CAMP) of the 21st century frontier R&D program funded by the Ministry of Commerce, Industry and Energy (MOCIE), Republic of Korea.

References

1. Hench LL (1998) J Am Ceram Soc 81:1705
2. Akao M, Aoki H, Kato K, Sato A (1982) J Mater Sci 17:243. doi:10.1007/BF00591468
3. Jarcho MH, Salsbury RL, Thomas J, Doremus RH (1979) J Mater Sci 14:142. doi:10.1007/BF01028337
4. Ryu HS, Hong KS, Lee JK, Kim DJ, Lee JH, Chang BS, Lee CH, Chung SS (2004) Biomaterials 25:393. doi:10.1016/S0142-9612(03)00538-6
5. Descamps M, Hornez JC, Leriche A (2007) J Eur Ceram Soc 27:2401. doi:10.1016/j.jeurceramsoc.2006.09.005
6. Lei Y, Rai B, Ho KH, Teoh SH (2007) Mater Sci Eng C 27:293. doi:10.1016/j.msec.2006.05.006
7. Biqiong C, Kang S (2005) Polymer Test 24:978. doi:10.1016/j.polymertesting.2005.07.013
8. Gain AK, Lee BT (2006) Mater Sci Eng A 419:269. doi:10.1016/j.msea.2005.12.033
9. Huang SG, Vleugels J, Li L, Biest OV, Wang PL (2005) J Eur Ceram Soc 25:3109. doi:10.1016/j.jeurceramsoc.2004.07.003
10. Lee BT, Kang IC, Cho SH, Song HY (2005) J Am Ceram Soc 88:2262
11. Lee BT, Youn MH, Paul RK, Lee KH, Song HY (2007) Mater Chem Phys 104:249. doi:10.1016/j.matchemphys.2007.02.009
12. Sabbagh J, Vreven J, Leloup G (2002) Dent Mater 18:64. doi:10.1016/S0109-5641(01)00021-5
13. Rezwan K, Chen QZ, Blaker JJ, Boccaccini AR (2006) Biomaterials 27:3413. doi:10.1016/j.biomaterials.2006.01.039